Targeted and random mutagenesis of cassava brown streak disease susceptibility factors reveal molecular determinants of disease severity

ZJ Daniel Lin[1,3], Myia K. Stanton[1], Gabriela L. Hernandez[1], Elizabeth J. De Meyer[1], Zachary von Behren[1], Katherine Benza[1,2], Helene Tiley[1], Emerald Hood[1], Greg Jensen[1], Kerrigan B. Gilbert[1], James C. Carrington[1], Rebecca S. Bart[1]

1. Donald Danforth Plant Science Center, Saint Louis, MO 63132, USA
2. Washington University, Saint Louis, MO 63130, USA
3. corresponding author: ZDL: dlin@danforthcenter.org

Abstract

Cassava brown streak disease (CBSD) is caused by cassava brown streak viruses (CBSVs) from the family *Potyviridae*. Potyvirid viral genome-linked protein (VPg) recruitment of host eukaryotic translation initiation factor 4E (eIF4E) proteins is a critical step in the viral life cycle. CBSV VPg interacts with all five cassava eIF4E-family members. Simultaneously knocking out *eIF4E*-family genes *nCBP-1* and *nCBP-2*, in cultivar 60444, strongly reduces CBSD root symptoms and viral titer but does not result in complete resistance, likely due to gene family redundancy. To test for redundancy, we generated single and double mutants for each clade of the *eIF4E* gene family in farmer preferred cultivar TME419. Double mutants for the *eIF(iso)4E* and *nCBP* clades both exhibited reduced symptom severity, with *ncbp-1 ncbp-2* having the strongest phenotype. A yeast two-hybrid screen for nCBP-2 mutants that lose VPg affinity identified fifty-one mutants, including an L51F mutant. This finding is consistent with one of the recovered cassava mutants that had a 6 amino acid deletion, including L51, in nCBP-2 and showed a reduction in symptoms relative to wild type. The data presented here suggest that generating mutations corresponding to L51F of nCBP-2 in multiple or all five cassava eIF4E proteins may lead to stronger resistance to CBSD while avoiding pleiotropic effects.

Keywords

Cassava brown streak disease, *Potyviridae*, eIF4E, viral genome-linked protein (VPg), gene editing, yeast two-hybrid

Introduction: 717
Results: 1,845
Discussion: 1,519
Materials & Methods: 1,263

Introduction

Cassava is one of the most important starch crops grown in the world (*Agricultural production statistics 2000–2022*, 2023). In sub-Saharan Africa, cassava is particularly important for food security, but its production is threatened by viral diseases (Rey & Vanderschuren, 2017). In particular, cassava brown streak virus (CBSV) and Ugandan cassava brown streak virus (UCBSV), closely related ipomoviruses belonging to the family *Potyviridae*, are of major concern (Tomlinson *et al.*, 2018; Robson *et al.*, 2023). Independent or simultaneous infection by these viruses cause cassava brown streak disease (CBSD). Symptoms of CBSD include feathery chlorosis of leaves, brown streaking of stems, and necrosis of storage roots. Cassava varieties with varying levels of resistance have been identified and are being deployed, but none of the varieties currently available to farmers are fully immune (Sheat & Winter, 2023; Robson *et al.*, 2023). A highly effective RNAi-based transgenic approach has been developed but faces regulatory hurdles in many target countries (Odipio *et al.*, 2014; Beyene *et al.*, 2016; Wagaba *et al.*, 2016; Tomlinson *et al.*, 2018).

Viruses of *Potyviridae* are positive sense, single stranded RNA viruses (Valli *et al.*, 2015). Many of these viruses have been studied extensively as a large number are agronomically important pests (Revers & García, 2015; Yang *et al.*, 2021). In many potyvirus-plant pathosystems, members of the host *eIF4E* gene family function as susceptibility factors and are necessary for completion of the viral life cycle (Robaglia & Caranta, 2006; Naderpour *et al.*, 2010; Hart & Griffiths, 2013; Bastet *et al.*, 2017; Gomez *et al.*, 2019; Gao *et al.*, 2020). This gene family encodes mRNA cap-binding proteins that facilitate recruitment of translation machinery to transcripts (Browning & Bailey-Serres, 2015). The plant *eIF4E*-family can be broken into three clades: *eIF4E*, *eIF(iso)4E*, and *nCBP* (Gomez *et al.*, 2019). Previous work in *Arabidopsis* demonstrated that turnip mosaic virus (TuMV) requires a functional copy of *eIF(iso)4E* for disease (Duprat *et al.*, 2002). Since then, potyvirus resistance loci in many crops have been mapped to *eIF4E*-family genes and alleles conferring potyvirus resistance often harbor missense mutations (Bastet *et al.*, 2017). Additional studies have demonstrated that potyvirid viral protein genome-linked (VPg) interacts with eIF4E-family proteins (Wittmann *et al.*, 1997; Schaad *et al.*, 2000) confirming that the interacting *eIF4E*-family member functions as a susceptibility factor (Yeam *et al.*, 2007; Charron *et al.*, 2008). Conversely, viral isolates that break *eIF4E*-family based resistance have been found to have accumulated compensating mutations in their VPg (Charron *et al.*, 2008; Gallois *et al.*, 2010; Li *et al.*, 2016; Lebaron *et al.*, 2016; Takakura *et al.*, 2018). VPg is covalently linked to the 5' end of the viral genome. It has been hypothesized that VPg interacts with eIF4E-family proteins to recruit translational machinery to synthesize the viral polypeptide (Sanfaçon, 2015) and complete the viral life cycle. Solving the structure of VPg-susceptibility factor protein complex could facilitate

76 engineering of susceptibility factor alleles that cannot be co-opted by the pathogen. However,
77 co-crystal structures have yet to be produced and the VPg protein complex with eIF4E-family
78 *S* factors falls below the current minimum size limit required for cryogenic electron microscopy.
79 To date, engineering synthetic *eIF4E* resistance alleles has involved transferring resistance-
80 conferring mutations from one pathosystem to another with some degree of success (Kim *et*
81 *al.*, 2014; Bastet *et al.*, 2018, 2019; Zafirov *et al.*, 2021).
82 We previously found that simultaneous mutations in two cassava eIF4E-family
83 members, *nCBP-1* and *nCBP-2,* strongly attenuated CBSD storage root necrosis and
84 accumulation of CBSV in storage roots of cultivar 60444 (Gomez *et al.*, 2019). Knocking out
85 *nCBP-2* alone resulted in an intermediate phenotype, while the *ncbp-1* single mutant exhibited
86 no differences from wild type. Aerial symptoms persisted in the *ncbp-1 ncbp-2* double mutant,
87 although with less severe stem brown streaking. This incomplete resistance suggests that VPg
88 may interact broadly with the remaining cassava eIF4E-family proteins. Indeed, CBSV VPg
89 could associate with all five cassava eIF4E-family proteins by coimmunoprecipitation (Gomez
90 *et al.*, 2019). As full CBSD resistance may require engineering all cassava *eIF4E*-family
91 alleles to evade CBSV VPg, we employed targeted and random mutagenesis of nCBP-2 to
92 identify structural determinants of VPg interaction. Furthermore, to better understand the
93 degree of functional redundancy exhibited by cassava eIF4E-family proteins in CBSD, we here
94 expand our CRISPR/Cas enabled genetic approach to characterize the roles of cassava eIF4E
95 and eIF(iso)4E clades in CBSD.
96
97 **Results**
98 **Generation of cassava *eIF4E*-family mutants**
99 We previously reported that a cassava *ncbp-1 ncbp-2* double mutant in the 60444
100 background displayed increased, but incomplete, resistance to CBSV challenge (Taylor *et al.*,
101 2012; Gomez *et al.*, 2019). While VPg interacted most strongly with nCBP-1 and nCBP-2 in
102 yeast two-hybrid assays, all five eIF4E-family proteins interacted with VPg in co-
103 immunoprecipitation assays. These results suggest that there is likely functional redundancy
104 among this family of proteins. To test this idea, we used CRISPR/Cas9-mediated genome
105 editing to generate new cassava *eIF4E*-family mutants in TME419, a farmer preferred cassava
106 cultivar. gRNAs were designed to target the first exon of each target gene and cassava
107 transformations were performed as previously described (Fig. S2) (Taylor *et al.*, 2012; Gomez
108 *et al.*, 2019). A total of 156 recovered lines from 21 transformations were characterized for
109 possible mutations at the target site(s) using amplicon sequencing. These efforts yielded
110 independent single mutant lines for all members of the cassava *eIF4E* gene family, along with
111 *eif(iso)4e-1 eif(iso)4e-2* and *ncbp-1 ncbp-2* double mutants (Table 1, S3). All but one mutant
112 line used in this study are predicted to have frameshifting mutations that result in loss of protein

113 function. The lone exception is one of the *ncbp-1 ncbp-2* double mutants where both *nCBP-1*
114 alleles and one allele of *nCBP-2* have frameshifting mutations and the remaining *nCBP-2*
115 allele has a deletion that results in loss of amino acids 45 through 51. This allele is designated
116 *nCBP-2*^{K45_L51del} and the mutant line is designated *ncbp-1 nCBP-2*^{K45_L51del} (Table 1, S3). No
117 differences in growth and development were observed between any of the mutant lines and
118 wild type (Fig. S3-4).
119
120 **CBSD phenotypes of TME419 *eIF4E*-family mutants**
121 To determine the contribution of cassava *eIF4E* family genes to development of CBSD,
122 mutant and wild type TME419 were challenged with CBSV isolate Naliendele in greenhouse
123 trials where stem brown streaking and leaf feathery chlorosis were tracked for approximately
124 three months. The specific CBSV isolate was chosen as it produces strong aerial symptoms
125 quickly after inoculation and reliably results in strong storage root necrosis (Wagaba *et al.*,
126 2013). At the end of the viral challenges, storage roots were excavated from soil, sectioned,
127 and scored for severity of necrosis as a measure of spread along storage root length and
128 diameter (Gomez *et al.*, 2019). These same root samples were used to measure viral titer by
129 quantitative real-time PCR (qRT-PCR). For aboveground symptoms, *eif4e*, *eif(iso)4e-1,*
130 *eif(iso)4e-2,* and *ncbp-1* single mutants had no reduction in disease severity relative to wild
131 type, while *ncbp*-2 and both *eif(iso)4e* and *ncbp* double mutants exhibited small but significant
132 reductions (Figure 1a). For storage root necrosis symptoms in the single mutants, the *ncbp-1*
133 and *ncbp-2* mutants displayed a decrease in symptoms compared to wild type with the latter
134 showing the strongest phenotype (Figure 1b). Each of the double mutants showed a decrease
135 in symptom with the *ncbp-1 ncbp-2* mutant, where all *nCBP* alleles have frameshifting
136 mutations, having the greatest reduction in necrosis; virtually no necrosis was observed
137 (Figure 1b, d). We further measured viral accumulation in storage roots of wild type, *ncbp-1*,
138 *ncbp-2*, *ncbp-1 ncbp-2*, and *ncbp-1 nCBP-2*^{K45_L51del} lines using qPCR analysis and observed
139 that lines with frameshifting mutations in *ncbp-2* had significantly lower virus titer (Figure 1c).
140 Taken together, these data suggest that while nCBP-2 is the primary contributor to root
141 disease severity, other eIF4E-family members may also contribute throughout the plant.
142
143 **Purified CBSV VPg and cassava eIF4E-family proteins interact *in vitro***
144 To further explore functional redundancy within the eIF4E-family with respect to CBSD
145 and, specifically, interaction with VPg, we used a biochemical approach. Using co-
146 immunoprecipitation, we previously demonstrated that CBSV VPg and cassava eIF4E-family
147 proteins form complexes in whole cell lysates using co-immunoprecipitation (Gomez *et al.*,
148 2019). However, these experiments did not address whether the proteins are directly
149 interacting or if another complex member is present and facilitating the protein-protein

150 association. Thus, we tested if VPg directly associates with eIF4E-family proteins in the
151 absence of additional factors using a GST pull-down experiment. GST-tagged cassava eIF4E-
152 family proteins and VPg, tagged with both 6xHis and 3xFLAG, were expressed in and purified
153 from *E. coli* (Figure S5). We found that CBSV VPg was pulled down by GST-tagged eIF4E,
154 nCBP-1, and nCBP-2 in comparison to GST alone (Figure 2a, b). Pulldown of VPg by GST-
155 tagged eIF(iso)4E-1 and eIF(iso)4E-2 was also tested but we observed inconsistent
156 enrichment of VPg by GST-eIF(iso)4E-1 & -2, relative to GST alone, across experimental
157 replicates.
158
159 **Targeted nCBP-2 mutations fail to disrupt interaction with VPg**
160 If CBSV VPg can coopt all cassava eIF4E-family proteins for completing the viral
161 lifecycle, engineering cassava to be resistant to CBSV may require identifying alleles of *eIF4E*-
162 family genes encoding mutations that disrupt VPg binding but still allow for translation-initiation
163 activity. In other plant-potyvirid pathosystems, specific mutations within eIF4E-family members
164 have proved sufficient to block interaction with VPg while maintaining normal protein function
165 (Figure 2c) (Ashby *et al.*, 2011; Kim *et al.*, 2014). One well studied example is TuMV VPg and
166 *Arabidopsis* eIF(iso)4E. In this system, mutation of a highly conserved tryptophan (W92L) and
167 semi-conserved lysine (K149E) in *Arabidopsis* eIF(iso)4E disrupts binding of TuMV VPg in
168 pull-down and co-immunoprecipitation experiments. Overexpression of this mutant *eIF(iso)4E*
169 allele in Chinese cabbage confers resistance to TuMV (Miyoshi *et al.*, 2006; Kim *et al.*, 2014).
170 To test the hypothesis that specific *eIF4E* gene family alleles might avoid VPg binding, we
171 took a yeast two-hybrid approach using different alleles of *nCBP-2*. We recapitulated the
172 W92L/K149E mutations from Arabidopsis eIF(iso)4E in cassava nCBP-2, resulting in nCBP-
173 $2^{W118L/N170E}$ (Figure 2d). Whereas the eIF(iso)$4E^{W92L/K149E}$ no longer associated with TuMV VPg
174 in a co-immunoprecipitation experiment (Figure 2e), we observed that CBSV VPg was
175 similarly present in both wild type nCBP-2 and nCBP-$2^{W118L/N170E}$ pull downs (Figure 2f). VPg
176 - nCBP-$2^{W118L/N170E}$ interaction was also observed through yeast two-hybrid assay (Figure 2g,
177 h).
178 TuMV and CBSV belong to two different genera of *Potyviridae*, *Potyvirus* and
179 *Ipomovirus*. It is possible that viruses from these distinct genera have evolved mechanistic
180 differences in how their VPg proteins interact with host eIF4E-family *S* factors. To determine
181 VPg protein conservation between potyviruses and ipomoviruses, VPg sequences from five
182 major potyvirus clades were aligned with VPg sequences from seven of the eight known
183 ipomovirus species (TomMMoV, SPMMV, SqVYV, CocMoV, CVYV, UCBSV, CBSV) (Figure
184 S6). Across all VPg sequences analyzed, several highly conserved residues are observed, as
185 are striking genus-specific differences; four stretches of amino acids are present only in one
186 genus or the other (pink boxes). One of these stretches coincides with an α-α loop in PVY VPg

187 thought to directly interact with the ventral side of eIF4E (Coutinho de Oliveira *et al.*, 2019); in
188 ipomoviruses this region is eight amino acids shorter. Additionally, a highly conserved
189 aspartate residue (D77) necessary for TuMV VPg interaction with *Arabidopsis* eIF(iso)4E
190 (Léonard *et al.*, 2000), is not present in ipomoviruses, indicating this residue may have a less
191 conserved role in interactions between ipomovirus VPgs and eIF4E-family proteins.
192
193 **A yeast two-hybrid screen identifies nCBP-2 mutants that lose VPg affinity**
194 Since mutations from the known Arabidopsis resistance allele did not block nCBP-2 –
195 VPg interaction, we performed a yeast two-hybrid screen for nCBP-2 mutants that lose affinity
196 for VPg (Figure 3a). Mutant *nCBP-2* amplicons were generated by error-prone PCR and
197 cloned into the bait vector by *in vivo* recombination in EGY48 yeast already containing both
198 *lacZ* reporter and VPg prey vectors (Figure 3a). From roughly 1000 yeast transformants, 51
199 *nCBP-2* mutants were isolated that lost interaction with VPg (Table 2, Table S4). Forty-eight
200 unique amino acid substitutions were observed across forty-six unique nCBP-2 mutants. Of
201 the unique mutants, 27 had mutations affecting a single residue or the introduction of a
202 frameshifting deletion while 19 contained two or three mutated residues. Nine residues were
203 isolated more than once, with up to three unique amino acid substitutions identified. Mutants
204 were then filtered to identify residues with varying degrees of conservation (Figure S7) across
205 cassava eIF4E-family proteins resulting in 15 being re-cloned and validated for loss of VPg
206 interaction in yeast using a quantitative β-galactosidase activity assay. All but two mutants,
207 nCBP-2^{L147H} and nCBP-2^{R196S}, were confirmed to confer total loss of β-galactosidase activity
208 in yeast and suggest commensurate loss of VPg affinity (Figure 3b, 5b, S8). The R196S
209 mutant yeast did not have any reduction of β-galactosidase activity relative to yeast expressing
210 wild-type nCBP-2, while L147H mutant yeast exhibited an intermediate reduction in β-
211 galactosidase activity. We further validated by western blot analysis that the yeast used for
212 two-hybrid experiments expressed nCBP-2 variants and CBSV VPg (Figure S8).
213
214 **Translation initiation activity of isolated nCBP-2 mutants**
215 Previous work with *Arabidopsis eif4e* or *eif(iso)4e* mutants suggested that both genes
216 were functionally redundant for translation initiation. However, *eif4e* mutants exhibit subtle
217 reductions in fertility and biomass in addition to delayed flowering time (Bastet *et al.*, 2017,
218 2018). Similarly, simultaneous knockout of tomato *eIF4E1* and *eIF4E2* incurs a growth penalty
219 (Gauffier *et al.*, 2016). T93C is a yeast *eif4e* mutant with chromosomal *eIF4E* replaced with
220 *LEU2* (Altmann *et al.*, 1989). This yeast strain can survive on galactose media due to a
221 plasmid-based *eIF4E* gene that is galactose inducible but is repressed in the presence of
222 glucose (Figure 4a). Coding sequences of nCBP-2 mutants confirmed to lose affinity for CBSV
223 VPg by quantitative yeast two-hybrid were cloned into pG1.1 under control of the constitutive

224 yeast GPD promoter and transformed into T93C. Transfer of these T93C transformants from
225 galactose- to glucose-containing media revealed that only three nCBP-2 mutants rescue loss
226 of *eif4e*: nCBP-2$^{A20T/H94Q/L200P}$, nCBP-2^{L51F}, and nCBP-2^{S138P} (Figure 4bc, 5cd).
227
228 **Mutating the conserved HPL motif of nCBP-2 can affect VPg binding and disease**
229 Among the three nCBP-2 mutants that retained translation initiation activity, nCBP-
230 2^{L51F} stood out as having a mutation in the highly conserved HPL motif. In yeast, this motif
231 participates in docking with eIF4G (Grüner *et al.*, 2016, 2018). In addition, this amino acid is
232 deleted in the nCBP-2^{K45_L51del} cassava mutant line that displayed increased resistance to
233 CBSD (Figure 5a). The HPL motif is found in many plant eIF4E-family proteins and as such,
234 a mutation of the leucine may be suitable for engineering resistance to other potyvirids. We
235 tested the nCBP-2^{K45_L51del} mutant for interaction with VPg by quantitative yeast two-hybrid.
236 Yeast expressing this mutant exhibited no β-galactosidase activity, like yeast expressing
237 nCBP-2^{L51F} (Figure 5b, S9a). We confirmed this implied loss of VPg interaction by observing
238 strongly reduced VPg binding in GST pulldowns with both mutant proteins (Figure 6).
239 However, comparing wild-type nCBP-2, nCBP^{L51F} and nCBP-2^{K45_L51del} for translation initiation
240 activity in T93C yeast (Δ*eif4e*) showed that while nCBP-2^{L51F} was able to rescue loss of *eIF4E*
241 in T93C it was to a lesser degree than wild type nCBP-2, and nCBP-2^{K45_L51del} was not able to
242 complement T93C (Figure 4d, e). Leucine 51 of nCBP-2 corresponds to leucine 28 within
243 *Arabidopsis* eIF(iso)4E. We hypothesized that recapitulating the L51F substitution in
244 *Arabidopsis* eIF(iso)4E would have the similar effects on TuMV VPg binding. Using the same
245 quantitative yeast two-hybrid approach as above we observed that the L28F mutation strongly
246 disrupted eIF(iso)4E interaction with TuMV VPg (Figure 7a, S9b). However, it is not able to
247 rescue T93C *eif4e* mutant yeast (Figure 7b, c).
248
249 **Discussion**
250 *Potyviridae* is the largest plant-infecting family of RNA viruses comprised of 249
251 viruses across 12 genera (Walker *et al.*, 2022). The genus *Potyvirus* is perhaps the best
252 studied as it contains 206 of the 249 known viruses belonging to the family *Potyviridae*. In
253 comparison, only eight species of viruses belonging to the genus *Ipomovirus* have been
254 identified and much less is known about molecular ipomovirus-host interactions (Dombrovsky
255 *et al.*, 2014). While the genome structure and genes encoded by potyviruses and ipomoviruses
256 are similar, and thus it is reasonable to expect a degree of conservation in virulence strategies,
257 it is also likely that differences have arisen given the evolutionary divergence of the two
258 genera. For CBSV in particular, we note that while eIF4E-family proteins are clear
259 susceptibility factors, the breadth of family members that contribute to disease appears
260 broader than typically found for potyviruses (Bastet *et al.*, 2017). Furthermore, while

261 resistance-conferring amino acid substitutions in eIF4E-family proteins have been effectively
262 transferred between potyvirus-pathosystems, we find in this study that *Arabidopsis* eIF(iso)4E
263 mutations that break TuMV VPg interaction fail to do so for the cassava nCBP-2 interaction
264 with CBSV VPg. These observations highlight the need for further characterization of
265 ipomovirus-host molecular interactions.

266 Structure-function analysis of VPg interaction with eIF4E-family susceptibility factors
267 would strongly benefit from crystal or cryo-EM structures of the complex; these have yet to be
268 successfully generated (Coutinho de Oliveira *et al.*, 2019). Most recently, an NMR approach
269 solved the structure of PVY VPg (Coutinho de Oliveira *et al.*, 2019). The PVY VPg and human
270 eIF4E interaction interface was also mapped through monitoring chemical shift perturbations
271 of either protein during NMR spectroscopy. It is unclear how well these findings will translate
272 to diverse potyvirid VPg interactions with cognate plant eIF4E-family proteins, especially for
273 the plant specific eIF(iso)4E clade and considering significant divergence of ipomovirus VPg
274 sequences from those of potyviruses. Thus far, attempts to design *eIF4E*-family resistance
275 alleles have relied on inference-based approaches (German-Retana *et al.*, 2008; Ashby *et al.*,
276 2011; Kim *et al.*, 2014; Bastet *et al.*, 2018, 2019; Zafirov *et al.*, 2021). In contrast, here we
277 utilize a loss-of-affinity screen of randomly mutagenized nCBP-2 variants to identify key
278 residues necessary for interaction with CBSV VPg. Only three nCBP-2 amino acid residues
279 that we found to be necessary for interaction with VPg had previously been described in
280 potyvirus-plant pathosystems. These amino acid residues, D106, V164, and R168 in nCBP-2,
281 are highly conserved across eIF4E-family proteins. In pepper, the *pvr1*^{2} allele of *eIF4E* is
282 responsible for resistance to isolates of PVY and TEV, and the amino acid corresponding to
283 nCBP-2 D106 is one of three causal amino acid substitutions (Kang *et al.*, 2005). That
284 aspartate in pvr1^{2} is substituted with asparagine (D to N). For cassava nCBP-2, two separate
285 D106 substitutions were observed; D106V and D106H, the latter of which co-occurred with an
286 A41T substitution. Only the nCBP-2^{D106V} mutant was tested for translation initiation activity and
287 was found deficient in rescuing T93C *eif4e* yeast. It is unclear if a D106N mutation in nCBP-
288 2, as found in pvr1^{2}, would similarly break VPg interaction while preserving its translation
289 initiation activity. nCBP-2 V164, where mutation to leucine disrupts CBSV VPg interaction,
290 corresponds to V167 in eIF4E of pea. The pea eIF4E^{V167A} variant confers resistance to PSbMV
291 and can rescue *eif4e* yeast. In contrast, cassava nCBP-2^{V164L} does not rescue T93C *eif4e*
292 yeast. Whether the V164A mutation in nCBP-2 would have the same effects as in pea eIF4E
293 is an open question. Lastly, for nCBP-2 R168, the previously described NMR structural study
294 demonstrated that corresponding residues in human eIF4E and wheat eIF(iso)4E are involved
295 in the interaction with *Potato virus Y* VPg (Coutinho de Oliveira *et al.*, 2019). Like nCBP-2^{D016V}
296 and nCBP-2^{V164L}, nCBP-2^{R168C} also failed to rescue T93C.

297 Of the fourteen nCBP-2 loss-of-VPg-interaction mutants that we tested for translation
298 initiation activity, eleven were nonfunctional. The three nCBP-2 variants that retained function
299 were nCBP-2$^{A20T/H94Q/A148V}$, nCBP-2^{L51F}, and nCBP-2^{S138P}. For nCBP-2 $^{A20T/H94Q/A148V}$, A20
300 resides outside of the conserved core of eIF4E family proteins while H94 and A148 are present
301 in alpha helices found on the dorsal side of nCBP-2; further work is required to identify which
302 individual or combination of these amino acids are required for CBSV VPg interaction. S138
303 is similarly located in a dorsal alpha helix while L51 is closer to the dorsal side and located N-
304 terminal of a beta strand. Evidence from a study on PVY VPg interaction with human eIF4E
305 indicates that VPg interfaces with the ventral side of eIF4E (Coutinho de Oliveira *et al.*, 2019).
306 If this also applies to CBSV VPg interaction with nCBP-2, the four aforementioned amino acid
307 residues likely affect VPg binding in an indirect manner. Of particular importance for this study,
308 the L51F substitution impacts the HPL motif, which was also affected in our cassava *ncbp-1*
309 *nCBP-2^{K45_L51del}* line. This enabled assessment of the importance of that motif for CBSD
310 symptom severity. Unlike nCBP-2^{L51F}, nCBP-2^{K45_L51del} did not rescue T93C *eif4e* deficient
311 yeast. Surprisingly, despite inability to strongly interact with VPg and complement *eif4e*
312 activity, the *ncbp-1 nCBP-2^{K45_L51del}* root disease phenotype was intermediate to wild type and
313 *ncbp-1 ncbp-2*, indicating that this mutant version of *nCBP-2* is sufficient for the development
314 of some disease symptoms. A similar result has also been observed in pea *eIF4E* mutants
315 where of eight mutants unable to rescue *eif4e* mutant yeast, two were still able to confer
316 susceptibility to PsbMV (Ashby *et al.*, 2011). In such mutants, it may be that low levels of
317 residual translation initiation activity are sufficient for completion of the viral life cycle.
318 In cassava the eIF4E-family has five members and we previously demonstrate that all
319 five proteins interact with CBSV VPg by co-immunoprecipitation (Gomez *et al.*, 2019). We now
320 find, through pulldown experiments with purified proteins, that nCBP-1, nCBP-2, and eIF4E
321 can directly interact with CBSV VPg. This validates our approach for identifying nCBP-2
322 residues crucial for VPg interaction. In contrast, our pulldown experiments with VPg and
323 eIF(iso)4E-1 and -2 were uninformative. It may be that the cassava eIF(iso)4E proteins have
324 lower affinity for CBSV VPg than the nCBPs and eIF4E, precluding detection of interaction via
325 GST pulldown. This is supported by our earlier work using yeast two-hybrid to dissect CBSV
326 VPg and cassava eIF4E-family interactions; there, the combination of CBSV VPg with
327 eIF(iso)4Es produced weaker reporter activity than when VPg was combined with nCBPs
328 (Gomez *et al.*, 2019). A more granular understanding of differences in cassava eIF4E-family
329 protein affinity for CBSV VPg may be achieved using techniques like surface plasmon
330 resonance or isothermal titration calorimetry (Upadhyay et al., 2024).
331 To determine the contribution of each *eIF4E*-family gene to CBSV symptoms, and
332 therefore the biological relevance of interaction with VPg, we have used CRISPR/Cas9 to
333 generate single mutants of all five genes, as well as some double mutants, in cassava variety

334 TME419. Notably, the *ncbp* double mutant has near total reduction of storage root necrosis,
335 commensurate with strong reductions in viral titer. Of the two *nCBP* genes, *nCBP-2* appears
336 to be the main driver for the improved disease response as evidenced by the results of the
337 single *nCBP* mutants, and that *nCBP-2* is more highly expressed than *nCBP-1* (Gomez *et al.*,
338 2019). As noted in our previous work, the expression difference between *nCBP-2* and *nCBP-*
339 *1* is even more pronounced in storage roots and may be the reason for differential disease
340 response in roots and aerial tissues of *ncbp-2* and *ncbp-1 ncbp-2* mutants (Gomez *et al.*,
341 2019). The disease data are consistent between mutants in both 60444 (Gomez *et al.*, 2019)
342 and TME419. Beyond the *nCBP* clade, the *eIF(iso)4E* clade appears to have a small
343 contribution to disease as aerial symptom severity and storage root necrosis is slightly reduced
344 when both *eIF(iso)4E-1* and *eIF(iso)4E-2* are simultaneously knocked out. This finding also
345 argues against the *ncbp-1 ncbp-2* root disease phenotype being simply due to additively
346 knocking out family members. It remains to be seen if higher order mutant combinations would
347 have an even greater effect on reducing CBSD disease severity. It will also be important to
348 test the utility of *ncbp-1 ncbp-2* mediated resistance against the natural diversity of cassava
349 brown streak viruses in field trials.
350 A key consideration going forward is that any benefits conferred by mutations in eIF4E-
351 family proteins with respect to viral resistance may also be accompanied by growth and
352 developmental penalties (Gauffier *et al.*, 2016, Bastet *et al.*, 2017). Of the four residues
353 identified in *nCBP-2* mutants that appear to avoid this penalty, three (L51, H94, and A148) are
354 conserved within all cassava eIF4E-family proteins and the fourth (S138) is conserved within
355 three members. Targeted base editing of some or all of these residues across the entire eIF4E-
356 family may allow for improved CBSV response while maintaining essential protein translation
357 functions. Indeed, we demonstrate here that transferring the L51F mutation from *nCBP-2* into
358 *Arabidopsis* eIF(iso)4E, as an L28F mutation, results in loss of affinity for TuMV VPg. As base
359 editing approaches mature alongside improvements with gene targeting, combining these
360 approaches with loss-of-VPg interaction screens may facilitate isolation and implementation
361 of novel *eIF4E*-family resistance alleles. This may allow for countering the edge viruses hold
362 in the host-pathogen evolutionary arms race.
363
364 **Materials and Methods**
365 **Plasmid vector construction**
366 gRNAs for CRISPR/Cas9-based mutagenesis of cassava *eIF4E*-family genes were
367 selected using the CRISPOR webtool (Concordet & Haeussler, 2018). Cas-OFFinder was
368 then used to screen gRNAs for off-target activity against a TME419 reference based genome
369 assembly produced using data (SRX1393295) from Bredeson et al. and the AM560-2 v6.0
370 reference genome (Table S1) (Bae *et al.*, 2014; Bredeson *et al.*, 2016). gRNAs with off-targets

371 containing less than 2-mismatches were excluded from consideration. Finally, gRNAs were
372 cloned into the pDIRECT 21C CRISPR binary vector as previously described by (Čermák *et*
373 *al.*, 2017).
374
375 **Plant transformation, genotyping, and growth parameters**
376 Cassava cultivar TME419 was transformed as previously described (Veley *et al.*,
377 2023). DNA was extracted from recovered transformants using the CTAB procedure. PCR
378 was then used to amplify 240 to 428 bp regions encompassing the gRNA binding sites. Purified
379 amplicons were sent to GENEWIZ for amplicon sequencing. Amplicon sequencing data was
380 analyzed using the CRIS.py python program (Connelly & Pruett-Miller, 2019). Plantlets of
381 transgenic lines were then maintained in tissue culture (Taylor *et al.*, 2012).
382
383 **Viral challenge and disease phenotyping**
384 Cassava disease challenges with CBSV isolate Naliendele, including inoculation,
385 aerial and below ground disease severity assessments, and qPCR-based quantification of
386 storage root viral titer, were carried out as described previously (Gomez *et al.*, 2019). For data
387 analysis, wild type disease severity was compared across all challenges and no significant
388 differences were found (Figure S1). Data for all challenges were then aggregated to increase
389 sample sizes for statistical analysis.
390
391 **Co-immunoprecipitation and GST-pulldown experiments**
392 Co-immunoprecipitation was performed as described previously (Gomez *et al.*, 2019).
393 For GST-pulldown experiments, cassava *eIF4E*-family genes in pENTR/D-TOPO, from
394 Gomez et al., were cloned into pDEST15 (Invitrogen) by Gateway recombination (Invitrogen).
395 pDEST15 encoding cassava *eIF4E*-family genes and pGEX-4T-1 (encoding unfused GST,
396 Cytiva) were transformed into BL21-AI E. coli (Invitrogen) and transformants were used to
397 start overnight seed cultures. Seed cultures were then used to inoculate 250 mL of LB broth.
398 Once inoculated cultures were grown to an OD600 of 0.4, IPTG (pGEX-4T-1) or arabinose
399 (pDEST15) were added to final concentrations of 0.5 mM or 0.2%, respectively, to induce
400 recombinant protein production. Induced cells were incubated for four hours at 28°C. Cells
401 were then pelleted and resuspended in 4 mL of lysis buffer (125 mM Tris, 150 mM NaCl, 1
402 mM DTT, 5 mM $MgCl_2$, 10 mM $CaCl_2$, pH 7.4) supplemented with 1X cOmplete protease
403 inhibitor (EDTA-free, Roche). Lysozyme (GoldBio) was added to a concentration of 1 mg/mL
404 and the mixture was allowed to incubate at room temperature for 15 minutes. 50 uL DNAse I
405 (Thermo) was then added to the mixture, followed by sonication on ice to ensure complete
406 lysis and elimination of DNA induced viscosity. The resulting cell lysate was centrifuged at
407 4°C, maximum speed, for 20 minutes. 3.5 mL of clarified lysate was transferred to a new tube

408 and EDTA was added to a final concentration of 1 mM. GST and GST-eIF4E proteins were
409 then purified from clarified lysate using glutathione magnetic agarose beads (Pierce)
410 according to manufacturer's protocol. Glutathione was removed from GST and GST-fusion
411 protein eluates by buffer exchange with Amicon Ultra centrifugal filters (Millipore). CBSV
412 6xHis-VPg-3xFLAG-6xHIS was produced and purified for pulldown experiments as described
413 in (Gomez *et al.*, 2019). GST pulldown was performed by mixing 3 ug of GST or GST-eIF4E
414 proteins with 3 ug of VPg and 10 uL of resuspended glutathione magnetic agarose beads
415 (Pierce) in buffer A (125 mM Tris, 150 mM NaCl, 10 mM DTT, 1 mM EDTA, pH 7.4)
416 supplemented with 1X cOmplete protease inhibitor (EDTA-free, Roche). Samples were
417 incubated at 4°C for one hour. Beads were then washed four times with buffer A and proteins
418 were eluted with Laemmli sample buffer for analysis by western blotting. Antibodies used in
419 this study are described in Table S2.

420 For comparison of VPg pulldown by nCBP-2 variants across experiments, nCBP-2 and
421 VPg eluate band intensities were first measured using Image Lab (Bio-Rad). Within an
422 experiment, eluate VPg band intensities were first adjusted to correct for differing pulldown
423 efficiencies of each nCBP-2 variant using the following equation where VPg_X is VPg band
424 intensity for sample X and GST_X is full length GST fusion protein band intensity for sample X:

425 $$VPg_{X,\ adjusted} = VPg_X\ adjusted\ for\ GST\ fusion\ protein\ pulldown\ efficiency = \frac{VPg_X}{\left(\frac{GST_X}{GST_{nCBP-2}}\right)}$$

426 Adjusted VPg intensities were then expressed relative to the VPg intensity of the wild-type
427 nCBP-2 sample for that experiment:

428 $$Normalized\ VPg_X = \frac{VPg_{X,\ adjusted}}{VPg_{nCBP-2,\ adjusted}} \times 100$$

429

430 **Yeast two-hybrid assays**

431 All yeast two-hybrid experiments were performed using the EGY48 strain harboring
432 the pSH18-34 *lacZ* reporter plasmid along with pJG4-5 and pEG202 bait and prey plasmids
433 (Golemis & Khazak, 1997). pJG4-5 *CBSV VPg* bait plasmid and pEG202 *nCBP-2* prey
434 plasmids were created by using In-Fusion cloning (Takara) to insert CBSV VPg or nCBP-2
435 coding sequences into pJG4-5 or pEG202 linearized with EcoRI and XhoI. For qualitative
436 yeast two-hybrid experiments, EGY48 pSH18-34 yeast transformed with bait and prey
437 plasmids were first selected for on SD –ura –trp –his media supplemented with 2% glucose
438 (Gietz & Schiestl, 2007). Transformants were then plated onto SD –ura –trp –his media
439 supplemented with 2% galactose, 1% raffinose, 1X BU salts, and X-gal. Blue/white screening
440 was performed three to four days later. Quantitative yeast two-hybrid was performed using a
441 spectrophotometric β-galactosidase activity assay (Amberg *et al.*, 2006).

442 To screen for nCBP-2 mutants that lose affinity for CBSV VPg, pEG202 *nCBP-2* was
443 used as template for mutagenic PCR (Genemorph II, Agilent). Primers immediately flanking
444 the second and penultimate codon of *nCBP-2*, preserving the start and stop codons during
445 mutagenic PCR, were used with the low mutation rate protocol from the Genmorph II kit
446 (Agilent). pEG202 empty vector was then digested with EcoRI and SacI and the fragment
447 containing the yeast *HIS* marker was gel purified (Qiagen). A third pEG202 fragment
448 containing the yeast 2μ origin of replication was produced by PCR with ends that overlap the
449 *nCBP-2* mutant amplicons and pEG202 *HIS* marker fragment by 30 base pairs; co-
450 transformation of all three fragments into yeast result in assembly of an intact pEG202 *nCBP-*
451 *2* plasmid through yeast recombinational cloning. Mutant *nCBP-2* amplicons, pEG202 *HIS*
452 fragment, and pEG202 2μ fragment were mixed in a 4:1:1 molar ratio and co-transformed into
453 EGY48 yeast harboring the pSH18-34 and pJG4-5 *CBSV VPg* plasmids. Transformed yeast
454 were directly plated onto SD –ura –trp –his media supplemented with 2% galactose, 1%
455 raffinose, 1X BU salts, and X-gal. Four days post transformation, white or light blue colonies
456 were restreaked onto a new plate for further visual assessment of reduced β-galactosidase
457 activity. The yeast were then checked by PCR for the presence of full length *nCBP-2* insert in
458 pEG202 using vector backbone specific primers. *nCBP-2* mutant alleles were then amplified
459 from insert positive yeast using Q5 Hot Start polymerase (NEB) and analyzed by Sanger
460 sequencing.
461
462 **Yeast *eif4e* complementation assay**
463 3xFLAG and nCBP-2 or mutant nCBP-2 coding sequences were cloned into pG1.1
464 linearized with NcoI and BamHI using In-Fusion (Takara) to produce pG1.1 *3xFLAG-nCBP-2*.
465 *3xFLAG* was amplified from pB7-HFC (Huang *et al.*, 2016) while *nCBP-2* variants were
466 amplified from pEG202 yeast two-hybrid plasmids. pG1.1 plasmids were then transformed into
467 the conditional yeast *eif4e* mutant strain T93C (*eif4e*::LEU2 *ura3 trp1 leu2* [pGAL1-eIF4E
468 *URA3*]) (Altmann *et al.*, 1989). Transformants were plated on SD –ura –trp dropout media
469 containing 2% galactose and 1% raffinose and allowed to grow for five to seven days. Colonies
470 of transformed yeast were then resuspended in sterile water and a ten-fold dilution series
471 ranging from OD600 = 10^{-1} through 10^{-4} was plated on SD –ura –trp dropout media containing
472 2% glucose to examine for rescue by pG1.1 encoded *eIF4E*-family gene variants. Plates were
473 imaged after 5-7 days.
474
475 **Acknowledgements**
476 We would like to thank the DDPSC PGF team for their hard work in caring for our
477 plants. We thank Claire Albin for her assistance with CBSV challenges and Nigel Taylor for
478 allowing us to use Taylor Lab greenhouse space. Yeast strain T93C, pG1.1 At_eIF4E1, and

479 pG1.1 empty vector were generously provided by Dr. Karen S. Browning. Z.D.L. would like to
480 thank Susan Lin, Wei-Yang Lin, Chun-Hwa Lin, and Jocelyn Lin for their love and support.
481 Z.D.L. was funded by USDA NIFA award 2019-67012-29626 and the Bill & Melinda Gates
482 Foudnation (OPP1125410, R.B.S., S.E.J., J.C.C.). E.J.D., Z.V.B., H.T., and E.H. were funded
483 by the DDPSC NSF-REU program, DBI-1659812, -2050394, -1659812, and -2244275,
484 respectively.
485

486 **Competing Interests**

487 None to declare.

488

489 **Author Contributions**

490 Conceptualization: Z.D.L.; Methodology: Z.D.L., J.C.C., R.S.B.; Investigation: Z.D.L.,
491 M.K.S., G.L.H., E.D.M., Z.V.B., K.B., H.T., E.H., G.J., K.B.G.; Visualization: Z.D.L.; Writing –
492 original draft: Z.D.L.; Writing – reviewing & editing: Z.D.L., K.B.G., J.C.C., R.S.B.

493

494 **Data Availability**

495 The source data for all results presented in this study are provided in accompanying
496 supplementary files.

497

498 **References**

499 ***Agricultural production statistics 2000–2022***. **2023**. Rome, Italy: Food & Agriculture
500 Organization of the United Nations (FAO).

501 **Altmann M**, **Sonenberg N**, **Trachsel H**. **1989**. Translation in Saccharomyces cerevisiae:
502 initiation factor 4E-dependent cell-free system. *Molecular and cellular biology* **9**: 4467–4472.

503 **Amberg DC**, **Burke DJ**, **Strathern JN**. **2006**. Assay of β-galactosidase in yeast:
504 Permeabilized cell assay. *CSH protocols* **2006**: db.prot4158.

505 **Ashby JA**, **Stevenson CEM**, **Jarvis GE**, **Lawson DM**, **Maule AJ**. **2011**. Structure-based
506 mutational analysis of eIF4E in relation to sbm1 resistance to pea seed-borne mosaic virus
507 in pea. *PloS one* **6**: e15873.

508 **Bae S**, **Park J**, **Kim J-S**. **2014**. Cas-OFFinder: a fast and versatile algorithm that searches
509 for potential off-target sites of Cas9 RNA-guided endonucleases. *Bioinformatics (Oxford,*
510 *England)* **30**: 1473–1475.

511 **Bastet A**, **Lederer B**, **Giovinazzo N**, **Arnoux X**, **German-Retana S**, **Reinbold C**, **Brault V**,
512 **Garcia D**, **Djennane S**, **Gersch S**, *et al.* **2018**. Trans-species synthetic gene design allows

513 resistance pyramiding and broad-spectrum engineering of virus resistance in plants. *Plant*
514 *biotechnology journal* **16**: 1569–1581.

515 **Bastet A**, **Robaglia C**, **Gallois J-L**. **2017**. EIF4E resistance: Natural variation should guide
516 gene editing. *Trends in plant science* **22**: 411–419.

517 **Bastet A**, **Zafirov D**, **Giovinazzo N**, **Guyon-Debast A**, **Nogué F**, **Robaglia C**, **Gallois J-L**.
518 **2019**. Mimicking natural polymorphism in eIF4E by CRISPR-Cas9 base editing is associated
519 with resistance to potyviruses. *Plant biotechnology journal* **17**: 1736–1750.

520 **Beyene G**, **Chauhan RD**, **Ilyas M**, **Wagaba H**, **Fauquet CM**, **Miano D**, **Alicai T**, **Taylor NJ**.
521 **2016**. A virus-derived stacked RNAi construct confers robust resistance to cassava brown
522 streak disease. *Frontiers in plant science* **7**: 2052.

523 **Bredeson JV**, **Lyons JB**, **Prochnik SE**, **Wu GA**, **Ha CM**, **Edsinger-Gonzales E**,
524 **Grimwood J**, **Schmutz J**, **Rabbi IY**, **Egesi C**, *et al.* **2016**. Sequencing wild and cultivated
525 cassava and related species reveals extensive interspecific hybridization and genetic
526 diversity. *Nature biotechnology* **34**: 562–570.

527 **Browning KS**, **Bailey-Serres J**. **2015**. Mechanism of cytoplasmic mRNA translation. *The*
528 *Arabidopsis book* **13**: e0176.

529 **Čermák T**, **Curtin SJ**, **Gil-Humanes J**, **Čegan R**, **Kono TJY**, **Konečná E**, **Belanto JJ**,
530 **Starker CG**, **Mathre JW**, **Greenstein RL**, *et al.* **2017**. A multipurpose toolkit to enable
531 advanced genome engineering in plants. *The plant cell* **29**: 1196–1217.

532 **Charron C**, **Nicolaï M**, **Gallois J-L**, **Robaglia C**, **Moury B**, **Palloix A**, **Caranta C**. **2008**.
533 Natural variation and functional analyses provide evidence for co-evolution between plant
534 eIF4E and potyviral VPg. *The Plant journal: for cell and molecular biology* **54**: 56–68.

535 **Concordet J-P**, **Haeussler M**. **2018**. CRISPOR: intuitive guide selection for CRISPR/Cas9
536 genome editing experiments and screens. *Nucleic acids research* **46**: W242–W245.

537 **Connelly JP**, **Pruett-Miller SM**. **2019**. CRIS.Py: A versatile and high-throughput analysis
538 program for CRISPR-based genome editing. *Scientific reports* **9**: 4194.

539 **Coutinho de Oliveira L**, **Volpon L**, **Rahardjo AK**, **Osborne MJ**, **Culjkovic-Kraljacic B**,
540 **Trahan C**, **Oeffinger M**, **Kwok BH**, **Borden KLB**. **2019**. Structural studies of the eIF4E-VPg
541 complex reveal a direct competition for capped RNA: Implications for translation.
542 *Proceedings of the National Academy of Sciences of the United States of America* **116**:
543 24056–24065.

544 **Dombrovsky A**, **Reingold V**, **Antignus Y**. **2014**. Ipomovirus--an atypical genus in the family
545 Potyviridae transmitted by whiteflies. *Pest management science* **70**: 1553–1567.

546 **Duprat A**, **Caranta C**, **Revers F**, **Menand B**, **Browning KS**, **Robaglia C**. **2002**. The
547 Arabidopsis eukaryotic initiation factor (iso)4E is dispensable for plant growth but required
548 for susceptibility to potyviruses. *The Plant journal: for cell and molecular biology* **32**: 927–
549 934.

550 **Gallois J-L**, **Charron C**, **Sánchez F**, **Pagny G**, **Houvenaghel M-C**, **Moretti A**, **Ponz F**,
551 **Revers F**, **Caranta C**, **German-Retana S**. **2010**. Single amino acid changes in the turnip
552 mosaic virus viral genome-linked protein (VPg) confer virulence towards Arabidopsis
553 thaliana mutants knocked out for eukaryotic initiation factors eIF(iso)4E and eIF(iso)4G. *The*
554 *Journal of general virology* **91**: 288–293.

555 **Gao L**, **Luo J**, **Ding X**, **Wang T**, **Hu T**, **Song P**, **Zhai R**, **Zhang H**, **Zhang K**, **Li K**, *et al.*
556 **2020**. Soybean RNA interference lines silenced for eIF4E show broad potyvirus resistance.
557 *Molecular plant pathology* **21**: 303–317.

558 **Gauffier C**, **Lebaron C**, **Moretti A**, **Constant C**, **Moquet F**, **Bonnet G**, **Caranta C**, **Gallois**
559 **J-L**. **2016**. A TILLING approach to generate broad-spectrum resistance to potyviruses in
560 tomato is hampered by eIF4E gene redundancy. *The Plant journal: for cell and molecular*
561 *biology* **85**: 717–729.

562 **German-Retana S**, **Walter J**, **Doublet B**, **Roudet-Tavert G**, **Nicaise V**, **Lecampion C**,
563 **Houvenaghel M-C**, **Robaglia C**, **Michon T**, **Le Gall O**. **2008**. Mutational analysis of plant
564 cap-binding protein eIF4E reveals key amino acids involved in biochemical functions and
565 potyvirus infection. *Journal of virology* **82**: 7601–7612.

566 **Gietz RD**, **Schiestl RH**. **2007**. Frozen competent yeast cells that can be transformed with
567 high efficiency using the LiAc/SS carrier DNA/PEG method. *Nature protocols* **2**: 1–4.

568 **Golemis EA**, **Khazak V**. **1997**. Alternative yeast two-hybrid systems. The interaction trap
569 and interaction mating. *Methods in molecular biology (Clifton, N.J.)* **63**: 197–218.

570 **Gomez MA**, **Lin ZD**, **Moll T**, **Chauhan RD**, **Hayden L**, **Renninger K**, **Beyene G**, **Taylor NJ**,
571 **Carrington JC**, **Staskawicz BJ**, *et al.* **2019**. Simultaneous CRISPR/Cas9-mediated editing
572 of cassava eIF4E isoforms nCBP-1 and nCBP-2 reduces cassava brown streak disease
573 symptom severity and incidence. *Plant biotechnology journal* **17**: 421–434.

574 **Grüner S**, **Peter D**, **Weber R**, **Wohlbold L**, **Chung M-Y**, **Weichenrieder O**, **Valkov E**,

575 **Igreja C**, **Izaurralde E**. **2016**. The structures of eIF4E-eIF4G complexes reveal an extended
576 interface to regulate translation initiation. *Molecular cell* **64**: 467–479.

577 **Grüner S**, **Weber R**, **Peter D**, **Chung M-Y**, **Igreja C**, **Valkov E**, **Izaurralde E**. **2018**.
578 Structural motifs in eIF4G and 4E-BPs modulate their binding to eIF4E to regulate translation
579 initiation in yeast. *Nucleic acids research* **46**: 6893–6908.

580 **Hart JP**, **Griffiths PD**. **2013**. A series of eIF4E alleles at the Bc-3 locus are associated with
581 recessive resistance to Clover yellow vein virus in common bean. *Theoretical and applied*
582 *genetics* **126**: 2849–2863.

583 **Huang H**, **Alvarez S**, **Bindbeutel R**, **Shen Z**, **Naldrett MJ**, **Evans BS**, **Briggs SP**, **Hicks**
584 **LM**, **Kay SA**, **Nusinow DA**. **2016**. Identification of evening complex associated proteins in
585 Arabidopsis by affinity purification and mass spectrometry. *Molecular & cellular proteomics:*
586 *MCP* **15**: 201–217.

587 **Kang B-C**, **Yeam I**, **Frantz JD**, **Murphy JF**, **Jahn MM**. **2005**. The pvr1 locus in Capsicum
588 encodes a translation initiation factor eIF4E that interacts with Tobacco etch virus VPg. *The*
589 *Plant journal: for cell and molecular biology* **42**: 392–405.

590 **Kelley LA**, **Mezulis S**, **Yates CM**, **Wass MN**, **Sternberg MJE**. **2015**. The Phyre2 web portal
591 for protein modeling, prediction and analysis. *Nature protocols* **10**: 845–858.

592 **Kim J**, **Kang W-H**, **Hwang J**, **Yang H-B**, **Dosun K**, **Oh C-S**, **Kang B-C**. **2014**. Transgenic
593 Brassica rapa plants over-expressing eIF(iso)4E variants show broad-spectrum Turnip
594 mosaic virus (TuMV) resistance. *Molecular plant pathology* **15**: 615–626.

595 **Lebaron C**, **Rosado A**, **Sauvage C**, **Gauffier C**, **German-Retana S**, **Moury B**, **Gallois J-L**.
596 **2016**. A new eIF4E1 allele characterized by RNAseq data mining is associated with
597 resistance to potato virus Y in tomato albeit with a low durability. *The Journal of general*
598 *virology* **97**: 3063–3072.

599 **Léonard S**, **Plante D**, **Wittmann S**, **Daigneault N**, **Fortin MG**, **Laliberté JF**. **2000**. Complex
600 formation between potyvirus VPg and translation eukaryotic initiation factor 4E correlates
601 with virus infectivity. *Journal of virology* **74**: 7730–7737.

602 **Li H**, **Kondo H**, **Kühne T**, **Shirako Y**. **2016**. Barley yellow mosaic virus VPg is the
603 determinant protein for breaking eIF4E-mediated recessive resistance in barley plants.
604 *Frontiers in plant science* **7**: 1449.

605 **Madeira F, Madhusoodanan N, Lee J, Eusebi A, Niewielska A, Tivey ARN, Lopez R,**
606 **Butcher S. 2024**. The EMBL-EBI Job Dispatcher sequence analysis tools framework in
607 2024. Nucleic acids research **52**: W521–W525.

608 **Miyoshi H**, **Suehiro N**, **Tomoo K**, **Muto S**, **Takahashi T**, **Tsukamoto T**, **Ohmori T**,
609 **Natsuaki T**. **2006**. Binding analyses for the interaction between plant virus genome-linked
610 protein (VPg) and plant translational initiation factors. *Biochimie* **88**: 329–340.

611 **Naderpour M**, **Lund OS**, **Larsen R**, **Johansen E**. **2010**. Potyviral resistance derived from
612 cultivars of Phaseolus vulgaris carrying bc-3 is associated with the homozygotic presence of
613 a mutated eIF4E allele. *Molecular plant pathology* **11**: 255–263.

614 **Odipio J**, **Ogwok E**, **Taylor NJ**, **Halsey M**, **Bua A**, **Fauquet CM**, **Alicai T**. **2014**. RNAi-
615 derived field resistance to Cassava brown streak disease persists across the vegetative
616 cropping cycle. *GM crops & food* **5**: 16–19.

617 **Revers F**, **García JA**. **2015**. Molecular biology of potyviruses. *Advances in virus research*
618 **92**: 101–199.

619 **Rey C**, **Vanderschuren H**. **2017**. Cassava mosaic and brown streak diseases: Current
620 perspectives and beyond. *Annual review of virology* **4**: 429–452.

621 **Robaglia C**, **Caranta C**. **2006**. Translation initiation factors: a weak link in plant RNA virus
622 infection. *Trends in plant science* **11**: 40–45.

623 **Robson F**, **Hird DL**, **Boa E**. **2023**. Cassava brown streak: A deadly virus on the move. *Plant*
624 *pathology*.

625 **Sanfaçon H**. **2015**. Plant translation factors and virus resistance. *Viruses* **7**: 3392–3419.

626 **Schaad MC**, **Anderberg RJ**, **Carrington JC**. **2000**. Strain-specific interaction of the tobacco
627 etch virus NIa protein with the translation initiation factor eIF4E in the yeast two-hybrid
628 system. *Virology* **273**: 300–306.

629 **Sheat S**, **Winter S**. **2023**. Developing broad-spectrum resistance in cassava against viruses
630 causing the cassava mosaic and the cassava brown streak diseases. *Frontiers in plant*
631 *science* **14**: 1042701.

632 **Takakura Y**, **Udagawa H**, **Shinjo A**, **Koga K**. **2018**. Mutation of a Nicotiana tabacum L.
633 eukaryotic translation-initiation factor gene reduces susceptibility to a resistance-breaking
634 strain of Potato virus Y. *Molecular plant pathology* **19**: 2124–2133.

635 **Taylor N**, **Gaitán-Solís E**, **Moll T**, **Trauterman B**, **Jones T**, **Pranjal A**, **Trembley C**,
636 **Abernathy V**, **Corbin D**, **Fauquet CM**. **2012**. A high-throughput platform for the production
637 and analysis of transgenic cassava (Manihot esculenta) plants. *Tropical plant biology* **5**:
638 127–139.

639 **Tomlinson KR**, **Bailey AM**, **Alicai T**, **Seal S**, **Foster GD**. **2018**. Cassava brown streak
640 disease: historical timeline, current knowledge and future prospects. *Molecular plant*
641 *pathology* **19**: 1282–1294.

642 **Upadhyay V, Lucas A, Patrick C, Mallela KMG. 2024**. Isothermal titration calorimetry and
643 surface plasmon resonance methods to probe protein-protein interactions. Methods (San
644 Diego, Calif.) **225**: 52–61.

645 **Valli A**, **García JA**, **López-Moya JJ**. **2015**. Potyviridae. *Encyclopedia of Life Sciences*: 1–
646 10.

647 **Veley KM**, **Elliott K**, **Jensen G**, **Zhong Z**, **Feng S**, **Yoder M**, **Gilbert KB**, **Berry JC**, **Lin Z-**
648 **JD**, **Ghoshal B**, *et al.* **2023**. Improving cassava bacterial blight resistance by editing the
649 epigenome. *Nature communications* **14**: 85.

650 **Wagaba H, Beyene G, Trembley C, Alicai T, Fauquet CM, Taylor NJ. 2013**. Efficient
651 transmission of cassava brown streak disease viral pathogens by chip bud grafting. BMC
652 research notes **6**: 516.

653 **Wagaba H**, **Beyene G**, **Aleu J**, **Odipio J**, **Okao-Okuja G**, **Chauhan RD**, **Munga T**, **Obiero**
654 **H**, **Halsey ME**, **Ilyas M**, *et al.* **2016**. Field level RNAi-mediated resistance to cassava brown
655 streak disease across multiple cropping cycles and diverse East African Agro-ecological
656 locations. *Frontiers in plant science* **7**: 2060.

657 **Walker PJ**, **Siddell SG**, **Lefkowitz EJ**, **Mushegian AR**, **Adriaenssens EM**, **Alfenas-**
658 **Zerbini P**, **Dempsey DM**, **Dutilh BE**, **García ML**, **Curtis Hendrickson R**, *et al.* **2022**.
659 Recent changes to virus taxonomy ratified by the International Committee on Taxonomy of
660 Viruses (2022). *Archives of virology* **167**: 2429–2440.

661 **Wittmann S**, **Chatel H**, **Fortin MG**, **Laliberté JF**. **1997**. Interaction of the viral protein
662 genome linked of turnip mosaic potyvirus with the translational eukaryotic initiation factor
663 (iso) 4E of Arabidopsis thaliana using the yeast two-hybrid system. *Virology* **234**: 84–92.

664 **Yang X**, **Li Y**, **Wang A**. **2021**. Research advances in potyviruses: From the laboratory bench
665 to the field. *Annual review of phytopathology* **59**: 1–29.

666 **Yeam I**, **Cavatorta JR**, **Ripoll DR**, **Kang B-C**, **Jahn MM**. **2007**. Functional dissection of
667 naturally occurring amino acid substitutions in eIF4E that confers recessive potyvirus
668 resistance in plants. *The plant cell* **19**: 2913–2928.

669 **Zafirov D**, **Giovinazzo N**, **Bastet A**, **Gallois J-L**. **2021**. When a knockout is an Achilles'
670 heel: Resistance to one potyvirus species triggers hypersusceptibility to another one in
671 Arabidopsis thaliana. *Molecular plant pathology* **22**: 334–347.

672

673 **Supporting information**

674 **Fig. S1** Wild type aerial and storage root disease scores across all challenges
675 **Fig. S2** gRNAs used in this study
676 **Fig. S3** *eIF4E*-family mutant cassava plants
677 **Fig. S4** Representative *eif(iso)4e-1 eif(iso)4e-2* double mutant and wild type TME419 six
678 weeks post transfer to soil
679 **Fig. S5** Purified proteins for GST pulldown assays
680 **Fig. S6** Alignment of ipomovirus and potyvirus VPg's show significant divergence in AA
681 sequences
682 **Fig. S7** Alignment of cassava eIF4E-family proteins
683 **Fig. S8** Quantitative yeast two-hybrid assay confirms loss-of-affinity screen results
684 **Fig. S9** Western blot analysis of yeast strains used for yeast two-hybrid experiments
685 **Table S1** TME419 gRNA off-target sites
686 **Table S2** Antibodies used in this study
687 **Table S3** Gene editing outcomes for TME419 eIF4E-family mutants
688 **Table S4** All nCBP-2 loss-of-VPg-affinity mutants identified by yeast two-hybrid
689

690 **Figure legends**

691 **Fig. 1 Endpoint CBSD storage root disease severity in cassava eIF4E-family mutants**
692 a, b) Endpoint aerial disease (a) and storage root necrosis (b) observed in cassava eIF4E-
693 family single and double mutants after challenge with CBSV isolate Naliendele. Data
694 presented are an aggregate from all experimental replicates. Leaf and stem disease
695 symptoms are evaluated separately on a 0-5 scale and then added together for a total aerial
696 symptom score. Storage root necrosis severity was scored on a 1 to 5 scale, 1 being
697 asymptomatic and 5 corresponding to severe necrosis throughout all storage roots of a
698 plant. Mann-Whitney U test was used to detect statistical differences with an alpha = 0.05. *

699 ≤ 0.05, ** ≤ 0.01, *** ≤ 0.001. Asterisks above boxplots denote differences from wild type,
700 while asterisks above brackets indicate differences between indicated genotypes.
701 c) qRT-PCR quantification of storage root CBSV viral levels from challenged mutants. CBSV
702 HAM1 was quantified relative to cassava PP2A to obtain HAM1 normalized relative
703 quantities (NRQs). HAM1 NRQs for each genotype are presented as relative to the mean of
704 wild type. Statistical differences were detected with the Mann-Whitney U test as described in
705 (a, b).
706 d) Representative storage root sections from wild type and ncbp-1 ncbp-2 #213 plants
707 challenged with CBSV. Scale bar denotes 1 cm.

708 **Figure 2. Interaction of GST-cassava eIF4E family proteins and CBSV VPg *in vitro***
709 a, b) GST-pulldown assays were performed with CBSV VPg-6xHis-3xFLAG and GST or
710 GST-tagged cassava eIF4E-family proteins. Proteins were expressed in and purified from *E.*
711 *coli*. Human (Hs) eIF4E was also tested in (a).
712 c) Model for eIF4E-mediated resistance against potyvirids. Cartoon depicts potyvirid
713 genome-linked VPg protein bound to eIF4E-family protein in order to cause disease, while
714 mutations that disrupt this interaction results in resistance.
715 d) Coimmunoprecipitation of YFP or YFP- eIF4E-family proteins with TuMV 6xHis-VPg-
716 6xHIS-3xFLAG. VPg was expressed in and purified from *E. coli* and then mixed with extract
717 from *N. benthamiana* leaves expressing YFP or YFP-fusion proteins.
718 e) *Arabidopsis* eIF(iso)4E residues 92 through 150 aligned with homologous regions of
719 cassava eIF4E-family proteins. W92 and K150, marked red, are necessary for interaction
720 with TuMV VPg. * indicates conservation across all aligned proteins, : indicates conservation
721 of amino acids with strongly similar properties, and . indicates conservation of amino acids
722 with weakly similar properties.
723 f) GST-pulldown assay as in a) and b) with CBSV VPg incubated with either GST, GST-
724 nCBP-2, and GST-nCBP-2$^{W118L/N170E}$.
725 g) Comparison of nCBP-2 and nCBP-2$^{W118L/N170E}$ interaction with CBSV VPg by quantitative
726 yeast two-hybrid assay.
727 h) Western blot analysis of nCBP-2 and VPg expression in yeast from g).

728 **Fig. 3 A yeast two-hybrid loss-of-affinity screen identifies nCBP-2 residues necessary**
729 **for VPg interaction**
730 a) Workflow for using a yeast two-hybrid approach to identify nCBP-2 mutants that lose
731 affinity for CBSV Naliendele VPg. The resultant pEG202 prey vector encodes nCBP-2 fused
732 to the LexA DNA binding domain. pJG4-5 encodes CBSV VPg fused to the B42
733 transcriptional activation domain. The EGY48 yeast strain used harbors the pSH18-34

734 reporter plasmid containing *lacZ* driven by the LexA operator.
735 b) Ventral and dorsal views of cassava nCBP-2 structure produced using the Phyre2 server
736 (Kelley *et al.*, 2015). nCBP-2 structure of amino acids 49 through 226 was predicted using
737 wheat eIF4E (PDB ID: 2IDR) as a template. Mutated amino acid residues in nCBP-2 mutants
738 that lose VPg affinity and either rescue or fail to rescue *eif4e* yeast are highlighted in green
739 and pink, respectively. W118 and N170, homologous with TuMV VPg interacting residues of
740 *Arabidopsis* eIF(iso)4E, are highlighted in blue.

741 **Fig. 4 T93C *eif4e* yeast complementation by *nCBP-2* mutants**
742 a) Schematic for testing translation initiation activity of *nCBP-2* variants expressed from the
743 pG1.1 plasmid in T93C *eif4e* conditional mutant yeast.
744 b) Left panels: T93C yeast transformed with pG1.1 empty vector or pG1.1 encoding various
745 eIF4E-proteins grown on SD dropout media supplemented with galactose allowing for
746 conditional expression of yeast eIF4E from the pGAL1-eIF4E plasmid. Right panels: same
747 yeast strains from left panel grown on dropout media supplemented with glucose, preventing
748 complementation by the pGAL1-eIF4E plasmid.
749 c) Western blot analysis of 3xFLAG tagged nCBP-2 variant expression in yeast strains used
750 in a). Coomassie stained membrane is presented for assessing loading control.

751 **Fig. 5 Effects of HPL motif mutation on nCBP-2 affinity for CBSV VPg and translation**
752 **initiation**
753 a) Alignment of human eIF4E protein sequence with variants of cassava nCBP-2. The
754 conserved HPL motif is boxed in red and the L51F mutation in nCBP-2 is highlighted in cyan.
755 Asterisks denote conserved amino acid residues.
756 b) Quantitative yeast two-hybrid analysis of CBSV VPg interaction with nCBP-2 variants.
757 c) T93C *eif4e* yeast transformed with pG1.1 encoding *Arabidopsis eIF4E1* or cassava *nCBP-*
758 *2* variants under the control of a constitutive promoter. nCBP-2 variants are N-terminally
759 tagged with 3xFLAG. The T93C yeast strain harbors a plasmid encoding galactose-inducible
760 and glucose-repressible yeast *eIF4E*.
761 d) Western blot analysis of nCBP-2 expression in yeast used in c). A segment of coomassie
762 stained membrane is presented for loading control.

763 **Fig. 6 nCBP-2^{K45_L51del} and nCBP-2^{L51F} exhibit reduced affinity for CBSV VPg, *in vitro***
764 a) GST pulldown experiment assessing the ability of GST-nCBP-2 variants to bind CBSV
765 VPg. Full-length protein eluate band intensities are presented underneath the eluate western
766 blots and are expressed relative to the sample with the strongest band intensity.
767 b) Analysis of eluate VPg band intensity across three GST-pulldown experiments. Band
768 intensities are normalized to account for differing amounts of GST-fusion protein pulled down

769 and expressed relative to VPg intensity in the GST-nCBP-2 sample.

770 **Fig. 7 Effects of mutating the HPL motif leucine in *Arabidopsis* eIF(iso)4E**

771 a) Quantitative yeast two-hybrid analysis of TuMV VPg interaction with wild type *Arabidopsis*
772 eIF(iso)4E alongside W92L/K149E and L28F mutants.
773 b) T93C *eif4e* yeast complementation assay with wild-type and mutant *eIF4E*-family genes
774 from *Arabidopsis* and cassava.
775 c) Western blot analysis of eIF(iso)4E and nCBP-2 variants from cells used in (b).

776

777

778

779

780

781

782

783

784

785

786

787

788

789

790

791

792

793

Table 1. TME419 CRISPR mutant genotypes

Line #	CRISPR target	Gene/allele	INDEL	Protein nomenclature
6-95	*eIF4E*	*A*	-2	S21*fsX1
		B	–	"
172	*iso4E1+2*	*iso4E1 A*	-1	A11PfsX17
		iso4E1 B	-2	A11HfsX9
		iso4E2 A	-2	I7RfsX29
		iso4E2 B	1	E8RfsX36
92	*iso4E1+2*	*iso4E1 A*	-2	A11HfsX9
		iso4E1 B	-1	A11PfsX17
		iso4E2 A	-2	I7RfsX29
		iso4E2 B	1	E8RfsX36
10-9	*iso4E2*	*A*	1	E8RfsX36
		B	–	"
3-29	*iso4E1*	*A*	-1	A11PfsX17
		B	–	"
93	*nCBP1*	*A*	1	S23YfsX4
		B	-2	S23TfsX3
4-53	*nCBP2*	*A*	1	T23NfsX8
		B	–	"
213	*nCBP1+2*	*nCBP1 A*	1	S23YfsX4
		nCBP1 B	–	"
		nCBP2 A	-4	T22HfsX10
		nCBP2 B	-2	T23IfsX7
40	*nCBP1+2*	*nCBP1 A*	1	S23YfsX4
		nCBP1 B	1	P24TfsX3
		nCBP2 A	-21	K45_L51del
		nCBP2 B	-1	A46LfsX31

Table 2. Summary of nCBP-2 mutants found to lose affinity for CBSV VPg

No. loss-of-affinity mutants	Nucleotide substitutions per mutant (mean)	Nucleotide deletions per mutant (mean)	Unique alleles	No. unique AA substitutions	Frameshift mutants (unique/total)	Stop-gain mutants	Redundant AA substitution occurrences	AA residues with multiple occurrences of substitutions
51	1.37	0.15	46	48 [a]	7/8	7	7	8

[a] non-synonymous mutations downstream of frameshifting INDELs or stop-gain mutations are not counted

800

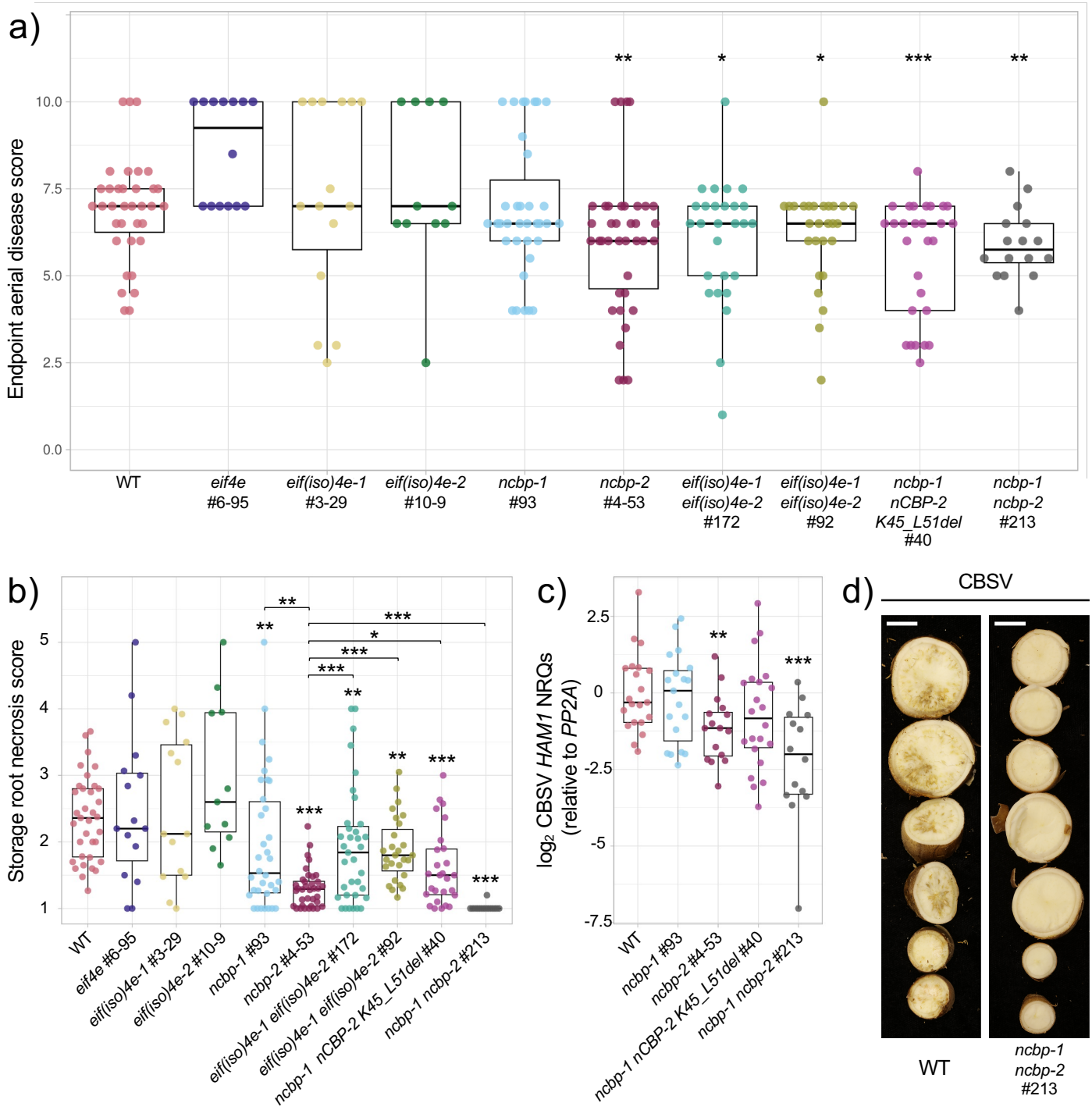

Fig. 1 Endpoint CBSD storage root disease severity in cassava *eIF4E*-family mutants

a, b) Endpoint aerial disease (a) and storage root necrosis (b) observed in cassava *eIF4E*-family single and double mutants after challenge with CBSV isolate Naliendele. Data presented are an aggregate from all experimental replicates. Leaf and stem disease symptoms are evaluated separately on a 0-5 scale and then added together for a total aerial symptom score. Storage root necrosis severity was scored on a 1 to 5 scale, 1 being asymptomatic and 5 corresponding to severe necrosis throughout all storage roots of a plant. Mann-Whitney U test was used to detect statistical differences with an alpha = 0.05. * ≤ 0.05, ** ≤ 0.01, *** ≤ 0.001. Asterisks above boxplots denote differences from wild type, while asterisks above brackets indicate differences between indicated genotypes.
c) qRT-PCR quantification of storage root CBSV viral levels from challenged mutants. CBSV *HAM1* was quantified relative to cassava *PP2A* to obtain *HAM1* normalized relative quantities (NRQs). *HAM1* NRQs for each genotype are presented as relative to the mean of wild type. Statistical differences were detected with the Mann-Whitney U test as described in (a, b).
d) Representative storage root sections from wild type and *ncbp-1 ncbp-2* #213 plants challenged with CBSV. Scale bar denotes 1 cm.

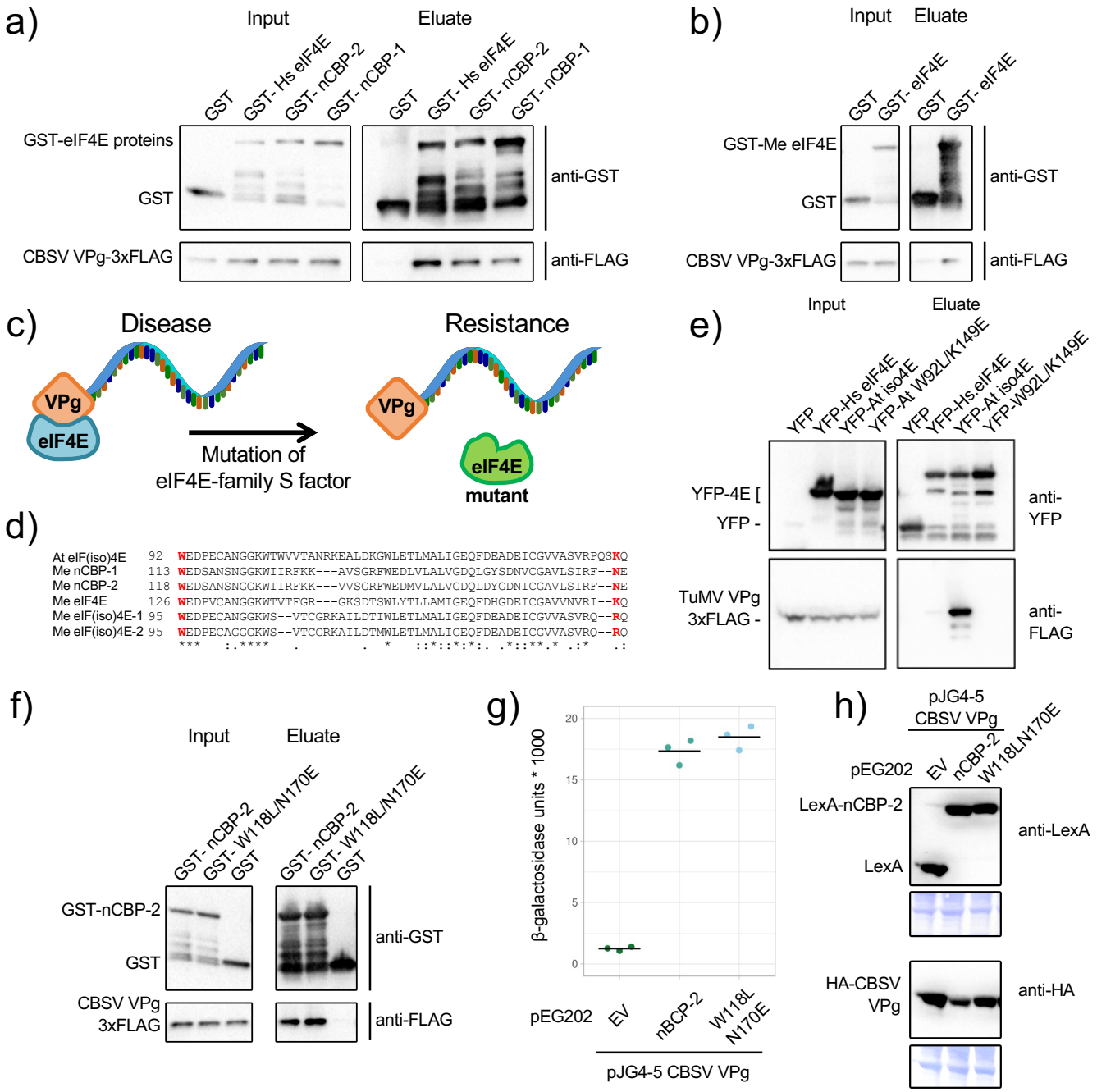

Figure 2. Interaction of GST-cassava eIF4E family proteins and CBSV VPg *in vitro*

a, b) GST-pulldown assays were performed with CBSV VPg-6xHis-3xFLAG and GST or GST-tagged cassava eIF4E-family proteins. Proteins were expressed in and purified from *E. coli*. Human (Hs) eIF4E was also tested in (a).
c) Model for eIF4E-mediated resistance against potyvirids. Cartoon depicts potyvirid genome-linked VPg protein bound to eIF4E-family protein in order to cause disease, while mutations that disrupt this interaction results in resistance.
d) Coimmunoprecipitation of YFP or YFP- eIF4E-family proteins with TuMV 6xHis-VPg-6xHIS-3xFLAG. VPg was expressed in and purified from *E. coli* and then mixed with extract from *N. benthamiana* leaves expressing YFP or YFP-fusion proteins.
e) *Arabidopsis* eIF(iso)4E residues 92 through 150 aligned with homologous regions of cassava eIF4E-family proteins. W92 and K150, marked red, are necessary for interaction with TuMV VPg. * indicates conservation across all aligned proteins, : indicates conservation of amino acids with strongly similar properties, and . indicates conservation of amino acids with weakly similar properties.
f) GST-pulldown assay as in a) and b) with CBSV VPg incubated with either GST, GST-nCBP-2, and GST-nCBP-2$^{W118L/N170E}$.
g) Comparison of nCBP-2 and nCBP-2$^{W118L/N170E}$ interaction with CBSV VPg by quantitative yeast two-hybrid assay.
h) Western blot analysis of nCBP-2 and VPg expression in yeast from g).

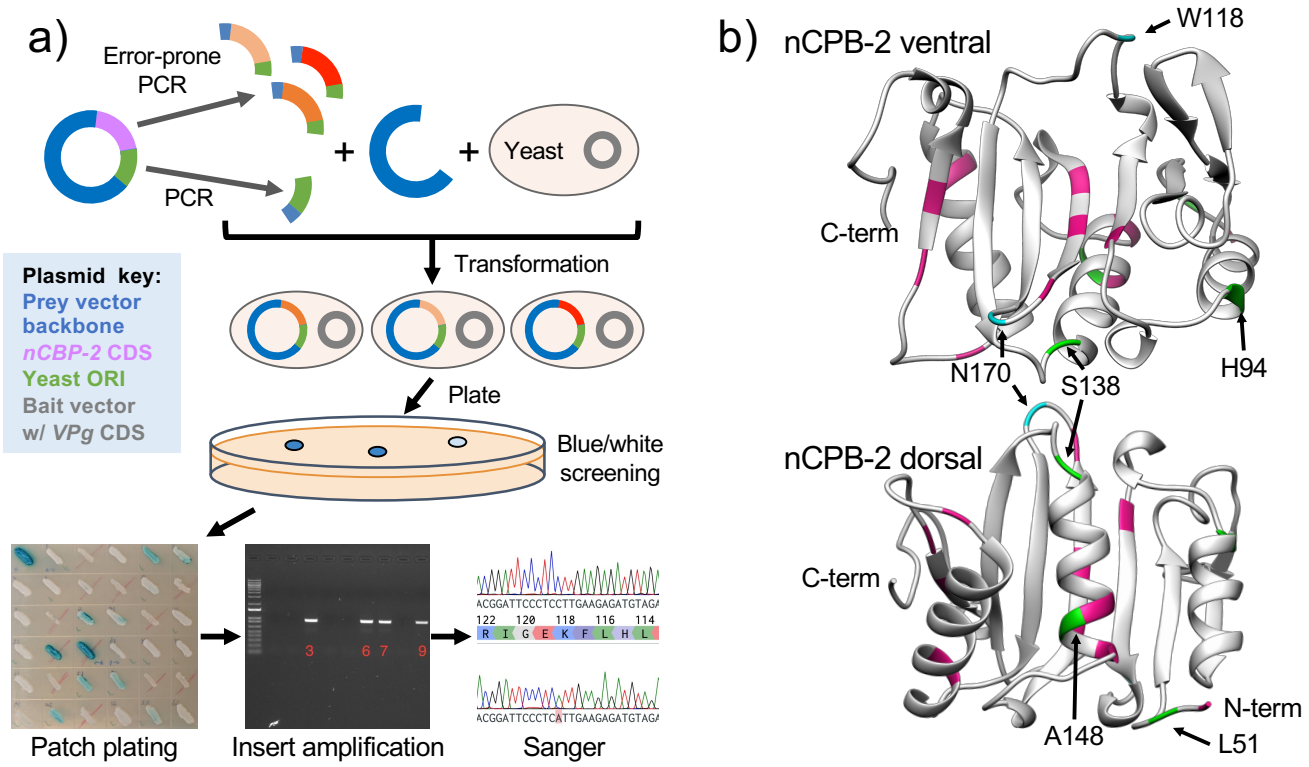

Fig. 3 A yeast two-hybrid loss-of-affinity screen identifies nCBP-2 residues necessary for VPg interaction

a) Workflow for using a yeast two-hybrid approach to identify nCBP-2 mutants that lose affinity for CBSV Naliendele VPg. The resultant pEG202 prey vector encodes nCBP-2 fused to the LexA DNA binding domain. pJG4-5 encodes CBSV VPg fused to the B42 transcriptional activation domain. The EGY48 yeast strain used harbors the pSH18-34 reporter plasmid containing *lacZ* driven by the LexA operator.
b) Ventral and dorsal views of cassava nCBP-2 structure produced using the Phyre2 server (Kelley LA et al., 2015). nCBP-2 structure of amino acids 49 through 226 was predicted using wheat eIF4E (PDB ID: 2IDR) as a template. Mutated amino acid residues in nCBP-2 mutants that lose VPg affinity and either rescue or fail to rescue *eif4e* yeast are highlighted in green and pink, respectively. W118 and N170, homologous with TuMV VPg interacting residues of *Arabidopsis* eIF(iso)4E, are highlighted in blue.

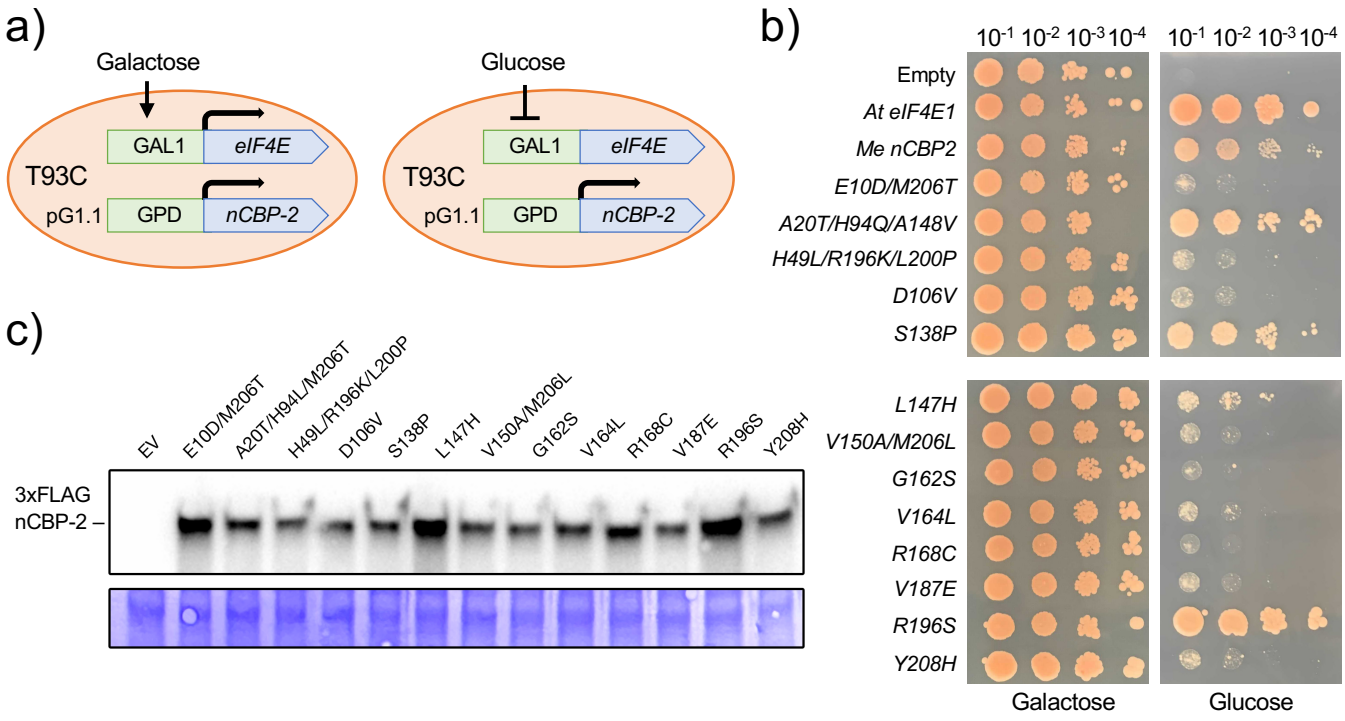

Fig. 4 T93C *eif4e* yeast complementation by *nCBP-2* mutants

a) Schematic for testing translation initiation activity of *nCBP-2* variants expressed from the pG1.1 plasmid in T93C *eif4e* conditional mutant yeast.
b) Left panels: T93C yeast transformed with pG1.1 empty vector or pG1.1 encoding various eIF4E-proteins grown on SD dropout media supplemented with galactose allowing for conditional expression of yeast eIF4E from the pGAL1-eIF4E plasmid. Right panels: same yeast strains from left panel grown on dropout media supplemented with glucose, preventing complementation by the pGAL1-eIF4E plasmid.
c) Western blot analysis of 3xFLAG tagged nCBP-2 variant expression in yeast strains used in a). Coomassie stained membrane is presented for assessing loading control.

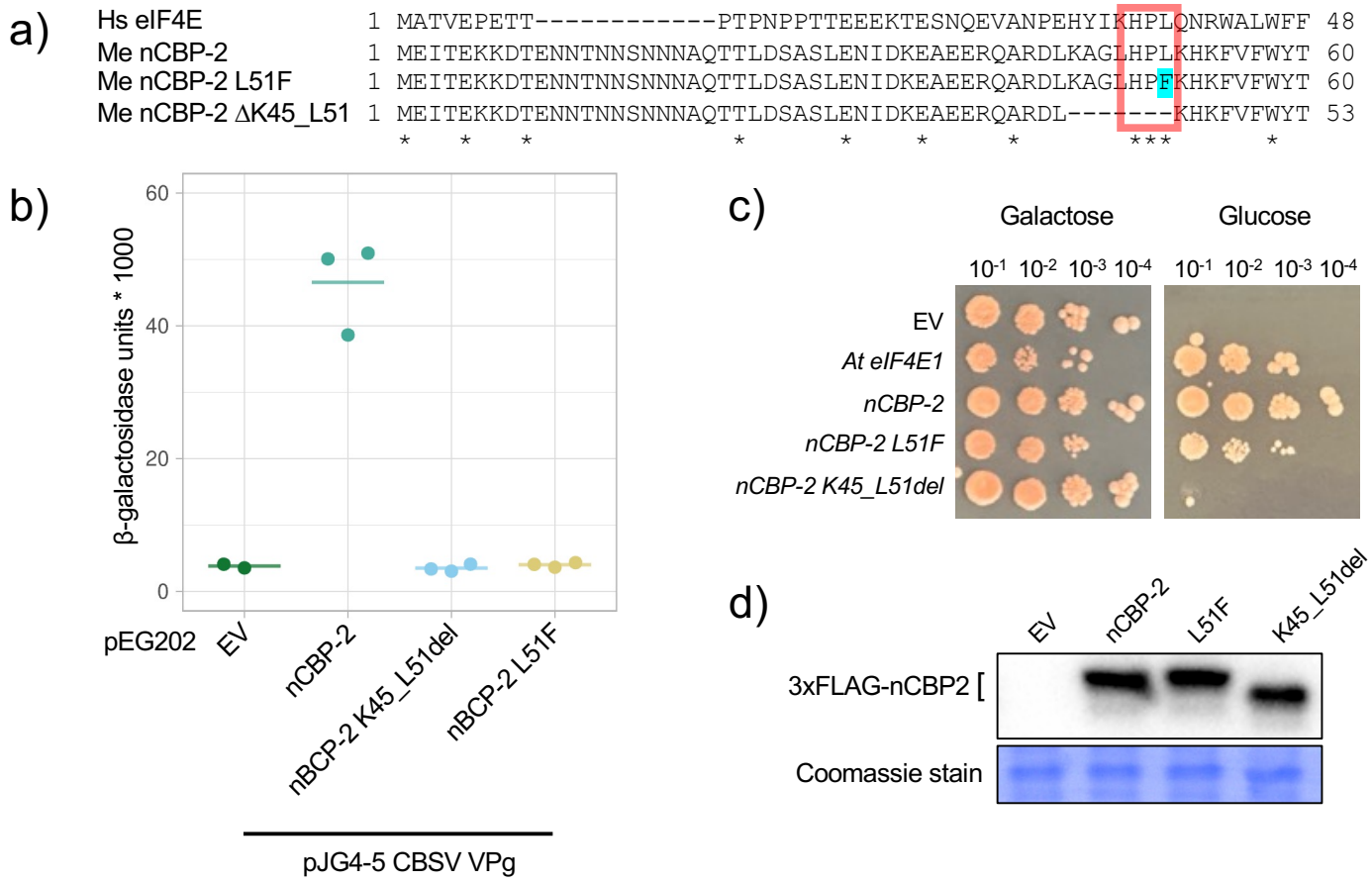

Fig. 5 Effects of HPL motif mutation on nCBP-2 affinity for CBSV VPg and translation initiation

a) Alignment of human eIF4E protein sequence with variants of cassava nCBP-2. The conserved HPL motif is boxed in red and the L51F mutation in nCBP-2 is highlighted in cyan. Asterisks denote conserved amino acid residues.
b) Quantitative yeast two-hybrid analysis of CBSV VPg interaction with nCBP-2 variants.
c) T93C *eif4e* yeast transformed with pG1.1 encoding *Arabidopsis eIF4E1* or cassava *nCBP-2* variants under the control of a constitutive promoter. nCBP-2 variants are N-terminally tagged with 3xFLAG. The T93C yeast strain harbors a plasmid encoding galactose-inducible and glucose-repressible yeast *eIF4E*.
d) Western blot analysis of nCBP-2 expression in yeast used in c). A segment of coomassie stained membrane is presented for loading control.

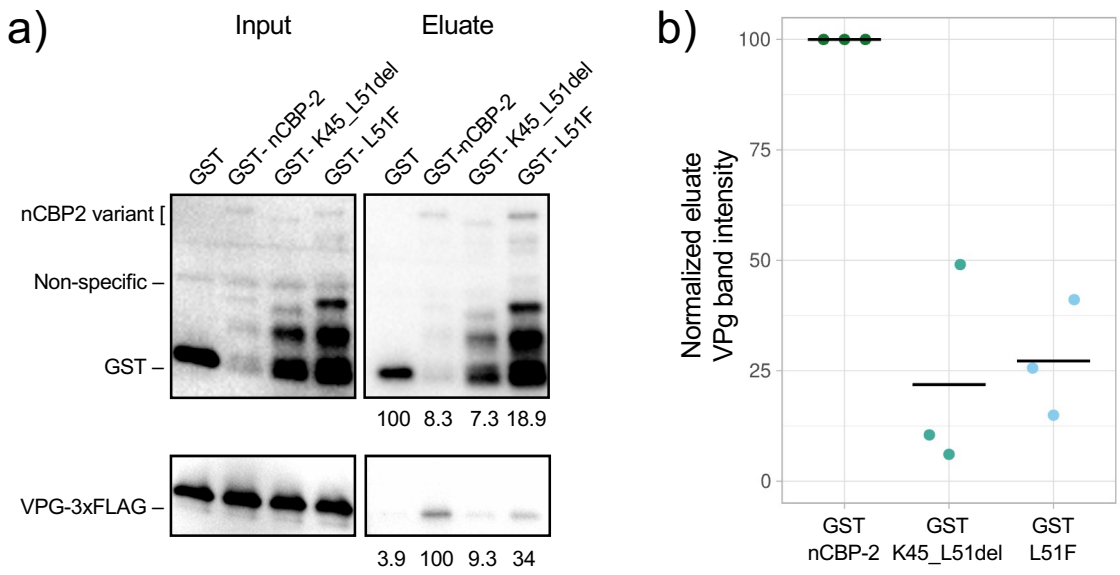

Fig. 6 nCBP-2^{K45_L51del} and nCBP-2^{L51F} exhibit reduced affinity for CBSV VPg, *in vitro*

a) GST pulldown experiment assessing the ability of GST-nCBP-2 variants to bind CBSV VPg. Full-length protein eluate band intensities are presented underneath the eluate western blots and are expressed relative to the sample with the strongest band intensity.
b) Analysis of eluate VPg band intensity across three GST-pulldown experiments. Band intensities are normalized to account for differing amounts of GST-fusion protein pulled down and expressed relative to VPg intensity in the GST-nCBP-2 sample.

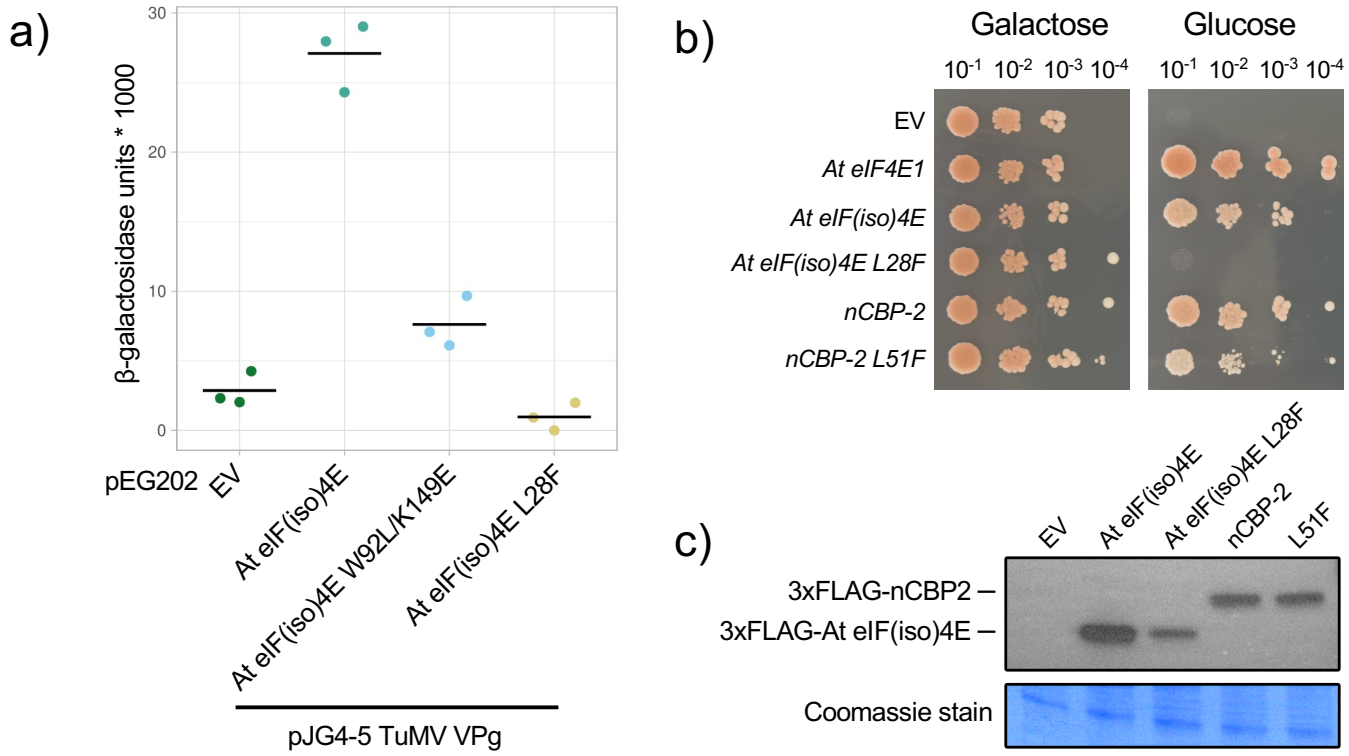

Fig. 7 Effects of mutating the HPL motif leucine in *Arabidopsis* eIF(iso)4E

a) Quantitative yeast two-hybrid analysis of TuMV VPg interaction with wild type *Arabidopsis* eIF(iso)4E alongside W92L/K149E and L28F mutants.
b) T93C *eif4e* yeast complementation assay with wild-type and mutant *eIF4E*-family genes from *Arabidopsis* and cassava.
c) Western blot analysis of eIF(iso)4E and nCBP-2 variants from cells used in (b).